Molecular Genetics and Metabolism Reports 20 (2019) 100478

Contents lists available at ScienceDirect

Molecular Genetics and Metabolism Reports

journal homepage: www.elsevier.com/locate/ymgmr

The mouse curly whiskers (*cw*) mutations are recessive alleles of hephaestin-like 1 (*Hephl1*)

Sidney Eragene, Jachius J. Stewart, Juan I. Samuel-Constanzo, Taotao Tan, Nia-Zaire Esgdaille, Krista J. Bigiarelli, Vanele D. DaCosta, Henry Jimenez, Thomas R. King*

Department of Biomolecular Sciences, Central Connecticut State University, 1615 Stanley Street, New Britain, CT 06053, USA

ARTICLE INFO

Keywords:
Positional-candidate approach
Meiotic backcross mapping
Hair morphology
Complementation testing
Splice-site mutation
Frameshift mutation

ABSTRACT

The spontaneous, curly whiskers mutation (abbreviated *cw*) generates kinky, brittle vibrissae in homozygous mice. Although *cw* has been mapped to the centromeric end of mouse Chromosome 9, no particular gene has been causally implicated, and this lack of genetic assignment has stymied *cw*'s complete molecular and functional analysis. As a foundation for its positional cloning, we have fine-mapped *cw* to a small, 0.57 Mb interval that contains only three skin-expressed genes, including hephaestin-like 1 (*Hephl1*), which encodes a membrane-bound, multi-copper ferroxidase. Sequence analysis of all *Hephl1* coding regions in *cw/cw* mutants revealed a single-base-pair substitution that alters *Hephl1* mRNA splicing, and is specific to the *cw* allele, only. Sequence analysis of a second, independent, re-mutation to curly whiskers (that we verified by complementation testing with *cw* and have designated cw^{2J}) revealed a distinct defect in *Hephl1* (a frame-shifting, single-base-pair insertion) that is specific to cw^{2J}. The results presented strongly suggest that defects in the *Hephl1* gene are the molecular basis of the classical, curly-whiskers mutant phenotypes.

1. Introduction

The recessive *cw* mouse mutation—named "curly whiskers" to highlight the most obvious mutant phenotype it controls—was discovered in 1958 in a subline of CBA/Cbi mice at the Chester Beatty Research Institute (London, UK), and its linkage with short ear (*Bmp5*) on Chromosome (Chr) 9 was first reported by Falconer and Isaacson [11,12]. The strongly curled vibrissae in mutants (see Fig. 1) are easily scored soon after birth, and persist throughout the life span. In 1967, Lyon and Butler [21] located *cw* very near the centromere on Chr 9, but this spontaneous variant has not been assigned to any causative gene. A distinct recessive mutation, initially named "tail hair depletion" (abbreviated *thd*), was reported by Les and Roths [20] to affect hair development in homozygotes while also generating a dominant, gain-type barrier to tail-skin graft compatibility. Mice carrying the *thd* mutation are now extinct, but while still extant this mutation was found (in a standard complementation test conducted by Roths) to be an allele of *cw*, and was renamed cw^{thd} in 1978.

These mutant phenotypes suggest that the gene identified by *cw* alleles must play important roles in both hair-follicle development and in histocompatibility. However, a detailed analysis of this pleiotropic locus has long been hampered by a lack of molecular probes that might allow interrogation of this gene's normal (and disrupted) structure and function. Here we have taken a positional-candidate approach [6] toward making such probes available. As a basis for this effort, we genetically mapped the original *cw* mutation to a very small interval on mouse Chr 9, where only three skin-expressed genes are also located. Next, DNA sequence analysis of one of those candidate genes in mice homozygous for *cw* or for a second, spontaneous, re-mutation to curly whiskers revealed distinct defects that are predicted to impair protein function. Taken together, the evidence we describe strongly suggests that these inherited defects in *Hephl1* (for hephaestin-like 1) are the molecular basis of the developmental and immunogenetic phenotypes displayed by the classical curly-whiskers mutants.

2. Materials and methods

2.1. Mice

Animals were housed and fed according to Federal guidelines, and the Institutional Animal Care and Use Committee (IACUC) at Central Connecticut State University (CCSU) approved of all procedures involving mice (Animal Protocol Applications #142, #158, #162 and #163). Mice from the standard inbred strains C57BL/6J (JAX Stock

* Corresponding author.
E-mail address: kingt@ccsu.edu (T.R. King).

https://doi.org/10.1016/j.ymgmr.2019.100478
Received 14 March 2019; Received in revised form 13 May 2019; Accepted 21 May 2019
Available online 20 June 2019

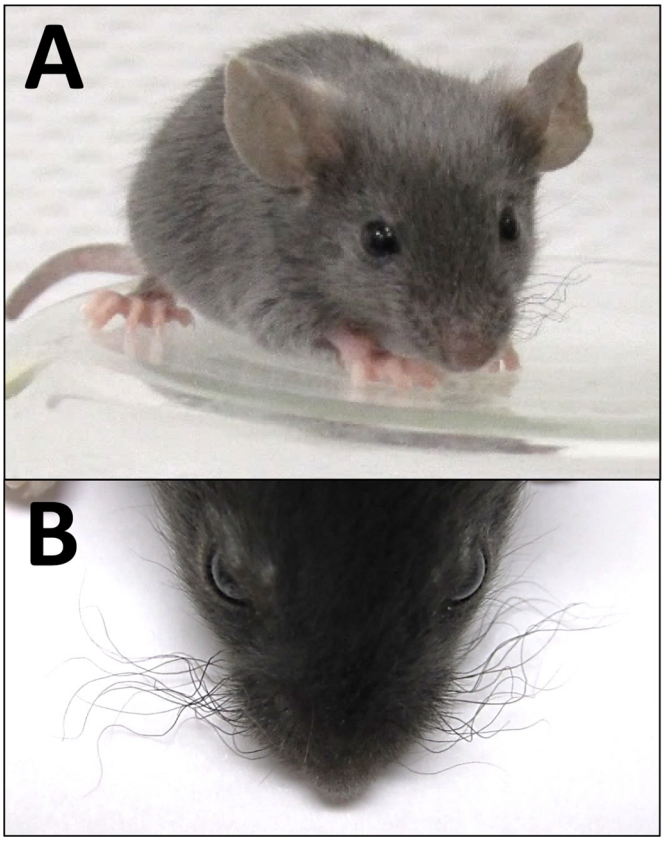

Fig. 1. The mutant curly whiskers phenotype. (A) A 25-day old CWD/LeJ mouse, homozygous for the *cw* mutation, and (B) a close-up of the mutant vibrissae.

#000664), C57BL/10SnJ (JAX Stock #000666), and DBA/2J (JAX Stock #000671); wild-derived, inbred CAST/EiJ mice (JAX Stock #000928); and inbred CWD/LeJ mice, homozygous for non-agouti (*a*), *cw*, and dilute (*Myo5a*^{d})(JAX Stock #000284) were obtained from The Jackson Laboratory (Bar Harbor, ME, USA). Although CWD/LeJ strain embryos were cryopreserved in 1989 and again in 1999 by crossing *cw Myo5a*^{d}/+ *Myo5a*^{d} with *cw Myo5a*^{d}/*cw Myo5a*^{d}, upon its most recent reconstitution in 2015, only *cw/cw* offspring were recovered, suggesting that the CWD/LeJ stock no longer segregates for *cw*, *cw*$^{+}$.

Twenty-four males of the strain B10.SM *H2*^{v} *H2-T18*^{b}/(70NS)Sn/J (JAX Stock #000456) were imported to CCSU (after cryo-recovery from liquid nitrogen storage since 1999) in June of 2018. These mice all displayed curly whiskers. In addition, we obtained (from Jane Ober, DNA Resource, The Jackson Laboratory, Bar Harbor, ME) DNA samples isolated from two, independent B10.SM *H2*^{v} *H2-T18*^{b}/(70NS)Sn/J mice that were archived in 1983 (without notation as to their whisker phenotype).

A frozen spleen sample (archived in 1999) from a mouse homozygous for the *cw-Bmp5*^{se}*-tk* haplotype—descended separately from the same, linkage-tester stock from which the CWD/LeJ line was derived in the 1960's—was kindly donated to us by Simon Ball and Rachel Summerfield (MRC Harwell, Oxfordshire, UK).

2.2. DNA isolation and analysis

Genomic DNA was isolated from two- to three-mm tail-tip biopsies taken from two- to three-week-old mice using Nucleospin® Tissue kits distributed by Clontech Laboratories, Inc. (Mountain View, CA, USA), as directed. The polymerase chain reaction (PCR) was performed in 13 µl reactions using the Titanium PCR kit from Clontech Laboratories, as directed. Oligonucleotide primers for PCR were designed and synthesized by Integrated DNA Technologies, Inc. (Coralville, IA, USA), based on sequence information available online [9,29]. To score PCR product sizes for microsatellite markers [8], reactions plus 2 µl loading buffer were electrophoresed through 3.5% NuSieve® agarose (Lonza, Rockland, ME, USA) gels. Gels were stained with ethidium bromide and photographed under ultraviolet light.

DNA markers based on single nucleotide polymorphisms (SNPs) previously reported to differ between wild-derived CAST and most standard inbred mouse strains [24] were also scored. These markers (herein designated *SNP1–5*) are described in detail in Supplementary Tables S1 and S2. For DNA sequence analysis, about 1.5 µg of individual PCR amplimers were purified and concentrated into a 30 µl volume using QIAquick® PCR Purification kits (Qiagen Sciences, Germantown, MD, USA) prior to primer-extension sequence analysis performed by the Keck Foundation Resource Laboratory at Yale University (New Haven, CT, USA).

To rapidly determine *cw* and *cw*^{2J} genotypes, especially in phenotypically wild type mice, 0.5 µg of individual PCR amplimers were purified and concentrated into a 30 µl volume using QIAquick® PCR Purification kits. For *cw* genotyping we used forward (5′ AAACGTGCT CTGAGATGG 3′) and reverse (5′GTTGCCTTGGAAATAAACTCC 3′) primers that flank the *Hephl1* splice-acceptor defect we describe in the text. For *cw*^{2J} genotyping we used forward (5′ ATCCAAGGCCTTCTGT TAAGG 3′) and reverse (5′CAGGATGGGACAGACTTTGG 3′) primers that flank *Hephl1*, Exon 14, which contains the single-base insertion we describe in the text. 12 ul samples of the respective purified amplimers were then incubated with 10 units of *Alu*I (for *cw* genotyping) or *Mly*I (for *cw*^{2J} typing) (New England BioLabs, Inc.; Ipswich, MA, USA) at 37 °C for 1 h prior to electrophoresis through 3.5% NuSieve® agarose gels at 145 V for 1 h.

2.3. RNA isolation and analysis

Total RNA was isolated from tail skin samples taken from 1-month-old mutant and control mice using the Nucleospin® RNA Midi kit by Macherey-Nagel (Bethlehem, PA, USA). From these samples, cDNA was generated using the SMARTer® RACE 5′/3′ kit (Clontech Laboratories, Inc.). To detect *Hephl1*-specific sequences, primer pairs that annealed in Exon 9 (5′-ACCTACAGGTGGACAGTGCCAGAAAGC-3′) and Exon 12 (5′-GCTGCTGATCTCATAGATCTGACCCATGCC-3′) were used to direct standard PCR amplifications of these cDNAs. Primers that annealed within Exon 4 of the mouse β actin (*Actb*) gene (5′-CCCAGCCATGAC GTAGCCATCCA-3′ and 5′-GAAGCTGTAGCCACGCTCGGTCAG-3′) were used together with *Hephl1* primers to provide an internal loading control. The resulting products were visualized in 3% NuSieve® agarose gels. For primer-extension sequencing, these amplification products were purified and concentrated (as described above) and shipped to the Keck Foundation Resource Laboratory at Yale University.

3. Results

3.1. Genetic mapping of the cw mutation on mouse Chr 9

To map the *cw* mutation with respect to molecular markers at the centromeric end of Chr 9, F_1 heterozygotes made by crossing CWD/LeJ-*cw/cw* mice with standard C57BL/6J mice were crossed back to CWD/LeJ mutants, producing 168 offspring. This intraspecific backcross (N_2) generation segregated for *cw*, dilute (*Myo5a*) and for several PCR-scorable, microsatellite DNA markers [8] on Chr 9. Supplementary Fig. S1 shows the string of markers transmitted by the F_1 parent to each of these 168 N_2 progeny. This haplotype analysis suggested that the *cw* gene must be located about 10% recombination centromeric to *D9Mit64*.

To more precisely locate *cw* in the region between *D9Mit64* and the centromere, a new set of F_1 heterozygotes was produced by crossing CWD/LeJ to the wild-derived CAST/EiJ strain (since this strain

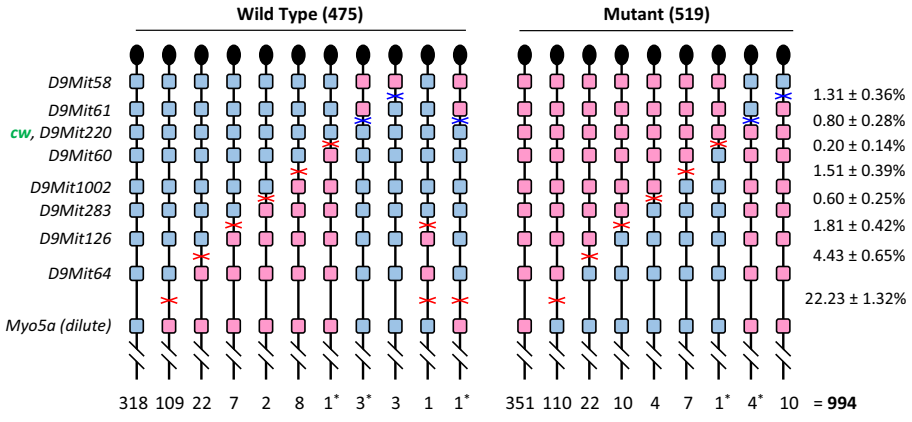

Fig. 2. Segregation of alleles of *cw*, *Myo5a* (dilute, *d*), and eight dimorphic microsatellite markers among 994 progeny from an inter-subspecific mouse backcross. Heterozygous F_1 mice (CWD/LeJ x CAST/EiJ) were backcrossed to homozygous CWD/LeJ mutants. The resulting progeny were scored for their fur texture and colour, and a DNA sample from each mouse was typed for the microsatellite markers shown at the left. Only the Chr 9 haplotype inherited from the F_1 parent is shown (with a knob at the top of the haplotype representing the centromere), and the number of mice inheriting that haplotype is shown below it. Very similar numbers of wild type and mutant progeny—as expected for a testcross ($\chi^2 = 1.95$, $P > .16$)—suggest that the mutant phenotype is both fully penetrant and fully viable. The five wild type and the five mutant recombinants marked with an asterisk show that the *cw* locus must lie between *D9Mit61* and *D9Mit60*. *D9Mit220* was not separated from *cw* in this backcross analysis. Genetic distances in percentage recombination are shown to the right (± 1 Standard Error).

combination offered more microsatellite and single-nucleotide marker dimorphisms than did the CWD/LeJ and C57BL/6J strain-pair), and these *cw*/+ heterozygotes were crossed back to CWD/LeJ mutants. The 994 N_2 progeny resulting from this inter-subspecific backcross were typed for curly whiskers, dilute pigmentation, and for 10 microsatellite markers on proximal Chr 9, as summarized in Fig. 2. This haplotype analysis indicated that *cw* must lie between markers *D9Mit61* and *D9Mit60*, and very close to marker *D9Mit220* (which was never meiotically separated from *cw* in this large backcross panel).

DNA samples from the ten mice identified as having a crossover between *D9Mit61* and *cw* or between *cw* and *D9Mit60* were typed next for five, single-nucleotide polymorphisms (SNPs) known to lie in the *D9Mit61* to *D9Mit60* interval. These five SNP markers are described in detail in Supplementary Tables S1 and S2, and are designated herein as *SNP1–5*. This analysis located the eight crossovers that fell centromeric to *cw* between *SNP1* and *SNP2*, and the two crossovers that fell distal to *cw* between *D9Mit220* and *SNP4* (see Fig. 3A), thus restricting the possible location of *cw* between *SNP1* and *SNP4* (very near *SNP2*, *SNP3* and *D9Mit220*, which were not meiotically separated from each other or from *cw*).

3.2. Evaluation of Hephl1 as the possible genetic basis of the cw mutation

The 0.57 Mb span from *SNP1* to *SNP4* (where the *cw* mutation must lie) includes ten expressed genes (Fig. 3A). Of these ten, at least six (*Piwil4*, *Fut4*, *Mre11a*, *Gpr83*, *Izumo1r* and *Panx1*) have been knocked out genetically with no reported effect on hair morphology ([2,3,14,15,32,33], respectively), making them unlikely to harbor a mutation that causes the curly-whiskers mutant phenotype. Of the remaining four genes, only three (*1700012B09Rik*, *Ankrd49* and *Hephl1*) are known to be expressed in skin [7], where the *cw* mutation has its most obvious effect in mouse mutants. Among these three, *Hephl1* [5] seemed to us the most likely gene candidate, since: 1) its product is expressed on the cell surface, where Les and Roths [20] suggested the histo-antigenic cw^{thd} gene product should be found; and 2) its product is a copper-dependent ferroxidase, and generalized copper deficiency (as in humans with defects in the Cu^{2+}-transporting ATPase, alpha polypeptide gene, *ATP7A*) is known to cause clinical features that include kinky hair [27].

To test this prime candidate further, the genomic DNA sequence of all *Hephl1* coding regions was determined for CWD/LeJ-*cw*/*cw* mutants and for C57BL/6 J control mice. This analysis revealed only a single-base difference in mutants compared to wild type: an A-to-G transition two bases upstream of Exon 11 (see Fig. 4A). Because this mutation appears to destroy a splice-acceptor signal, we generated cDNA from tail-skin transcripts isolated from *cw*/*cw* and control wild type tail skin, and PCR-amplified *Hephl1* sequences between Exon 9 and Exon 12. As shown in Fig. 4B, amplification of cDNA from wild-type skin yielded a 606 bp amplimer as expected for the normal splicing of Exons 9 through 12 (and see sequence details in Supplementary Fig. S2A). By contrast, amplification of *Hephl1* sequences from *cw*/*cw* skin-derived cDNA yielded two smaller PCR products of 581 and 393 bp (Fig. 4B). Primer-extension analysis of the 581 bp splice variant (Variant 1) revealed a novel junction between Exon 10 and a cryptic splice-acceptor site within Exon 11. This truncated Exon 11, designated Exon 11(Δ25), is 25 nucleotides shorter than the standard exon. This aberrant splice is predicted to disrupt the reading frame and alter three amino acids before an out-of-frame stop codon would terminate translation (as shown in Supplementary Fig. S2B). Primer-extension analysis of the 393 bp splice variant (Variant 2) showed Exon 10 joined with Exon 12 (see Supplementary Fig. S2C). The skipping of Exon 11 in this *cw*-specific transcript is predicted to omit 71 amino acids from the mutant protein product but maintain the normal downstream reading frame. The full-length wild-type and two, *cw*-specific, variant *Hephl1* transcripts are diagrammed in Fig. 3B.

Next, we developed an *Alu*I-sensitivity assay (see Supplementary Fig. S3A) that was used to rapidly screen among 57 mouse strains that are not associated with the *cw* mutation, and found the standard splice-acceptor sequence in all of them. Only one strain, a linkage-tester stock homozygous for the *cw-Bmp5*^{se}*-tk* haplotype (from the MRC Harwell Institute, Oxfordshire, UK), was found to encode the same *Hephl1* DNA defect as the CWD/LeJ strain (see Supplementary Fig. S3B & C).

3.3. Rediscovery and genetic characterization of the cw^{2J} mutation

One strain cryopreserved at The Jackson Laboratory, B10.SM *H2*^{v} *H2-T18*^{b}/(70NS)Sn/J (a C57BL/10 strain congenic for a recombinant *H2* haplotype), was described in some records (but not others) as carrying the *cw* mutation. We obtained DNA samples from two independent mice from this strain that were archived in 1983 (without notation as to their whisker phenotype), but these both showed the wild type sequence at the splice-acceptor site 5′ to Exon 11 in *Hephl1* (see Supplementary Fig. S3B & C). To determine whether B10.SM *H2*^{v} *H2-T18*^{b}/(70NS)Sn/J stock that was cryopreserved in 1994 might carry the *cw* mutation, we obtained 24 reconstituted males—which all displayed curly whiskers—and crossed some with known *cw* homozygotes or heterozygotes (see Table 1). The failure of a recessive defect homozygous in the B10.SM *H2*^{v} *H2-T18*^{b}/(70NS)Sn/J strain to complement *cw* (see Fig. 5) suggests that this defect is an allele of *cw*. Because this congenic strain is unrelated to the original *cw* mutation (and because it lacks the point mutation we have found to be specifically associated with *cw*), we hypothesized that this recessive variant might be a

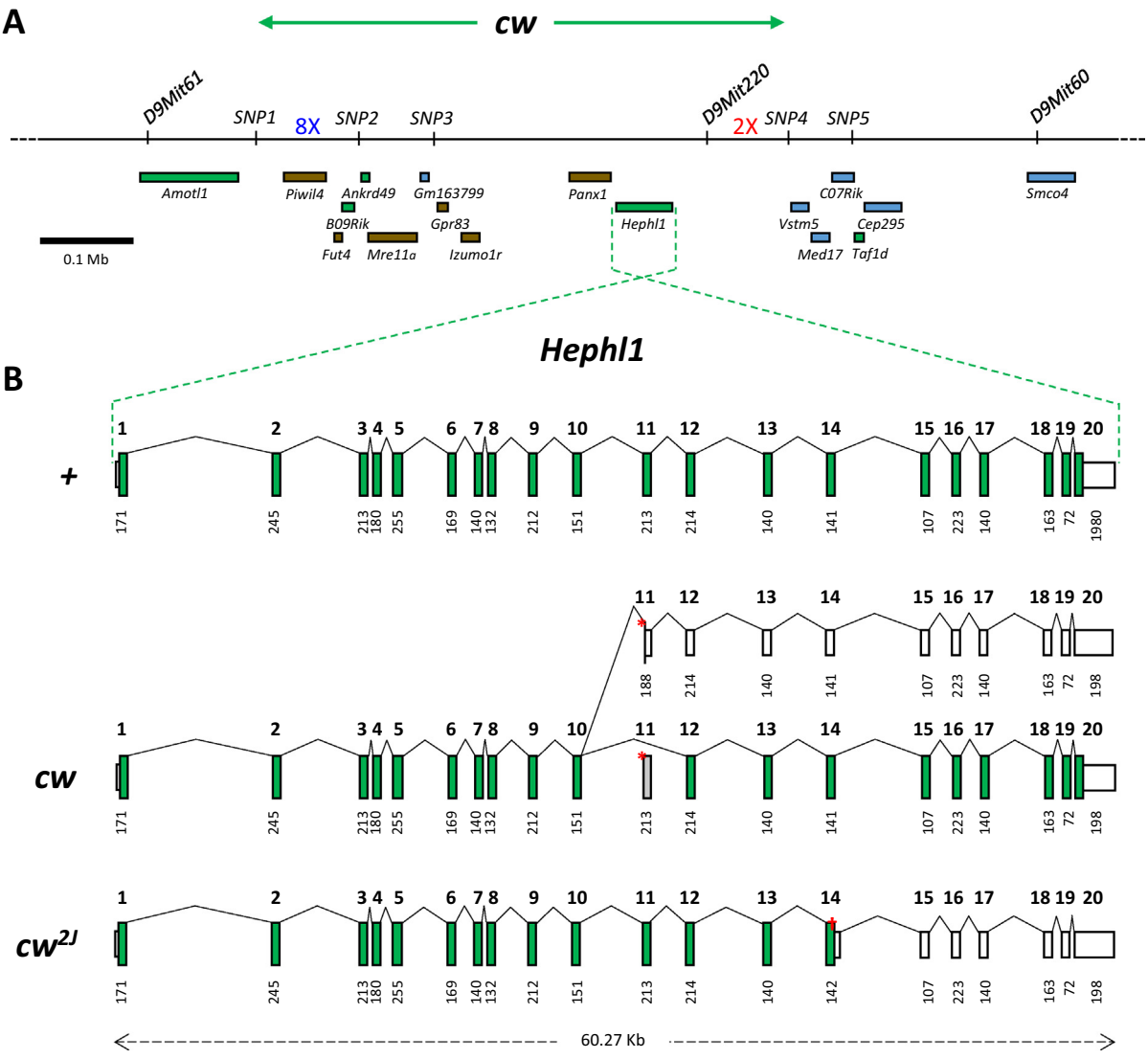

Fig. 3. Physical maps of the *cw*-critical region on mouse Chr 9. (A) The relative positions of three microsatellite (*D9Mit*) markers and five single-nucleotide (*SNP*) markers that closely flank *cw* are shown with a 0.1 Mb scale bar. The eight crossovers that fell centromeric to *cw* (shown in blue, and see Fig. 2) were localized between *SNP1* and *SNP2*, while the two crossovers that fell telomeric to *cw* (shown in red, and see Fig. 2) were located between *D9Mit220* and *SNP4*. The extent of 17 known genes that lie in the interval between *D9Mit61* and *D9Mit60* are shown below the line that represents Chr 9. Null alleles of the six genes depicted in brown do not impact hair development in homozygotes. Of the remaining 11 genes, those depicted in blue are not expressed in skin. Because *cw* must be located in the 0.57 Mb interval between *SNP1* and *SNP4*, the skin-expressed genes (*B09Rik*, *Ankrd4*, and *Hephl1*, depicted in green) are most likely to harbor the causative mutation. (B) The *Hephl1* gene is reversed and expanded to show the 20 exons it comprises. Tall green boxes represent coding regions and shorter white boxes represent the untranslated regions. The number below each exon is its length in base pairs. The mutant *Hephl1* allele found in *cw* mice is drawn to show a single-base-pair transition just 5′ to Exon 11 (indicated by the red asterisk) that eliminates a splice acceptor site, resulting in the two variant transcripts diagrammed here (and described further in the text). The mutant *Hephl1* allele found in cw^{2J} mice is drawn to show the insertion of a single A residue in Exon 14 (at the red dagger), that is predicted to generate an out-of-frame stop codon later in Exon 14 (as described further in the text). (For interpretation of the references to colour in this figure legend, the reader is referred to the web version of this article.)

spontaneous re-mutation that we designated “curly whiskers; curly whiskers 2 Jackson”, abbreviated cw^{2J}.

Sequence analysis of all 20 coding regions of the *Hephl1* gene in B10.SM $H2^{v}$ $H2\text{-}T18^{b}$/(70NS)Sn/J-cw^{2J} mutants revealed just one DNA defect *vs.* C57BL/10SnJ controls: the insertion of a single A residue in Exon 14, codon 820 (see Fig. 6A). This frameshift mutation is predicted to alter 7 amino acids before an out-of-frame stop codon would terminate translation. While normal-sized *Hephl1* PCR products may be amplified from cDNAs based on transcripts isolated from cw^{2J}/cw^{2J} mutant tail skin, those products appear less abundant than products amplified from cDNAs derived from wild-type skin (see Fig. 6B). This observation may indicate that cw^{2J} mutant transcripts are unstable, consistent with nonsense-mediated decay [4]. The full-length cw^{2J} transcript is diagrammed in Fig. 3B.

Finally, we developed an *Mly*I-sensitivity assay (see supplementary Fig. S4A) to rapidly screen among 60 mouse strains for defects in *Hephl1*, Exon 14, codon 820. The only amplimers resistant to endonuclease treatment (and verified by primer-extension analysis to possess an inserted adenosine residue) were based on our reconstituted B10.SM $H2^{v}$ $H2\text{-}T18^{b}$/(70NS)Sn/J-cw^{2J} mice or on the B10.SM $H2^{v}$ $H2\text{-}T18^{b}$/(70NS)Sn/J DNA samples that were archived in 1983 (see Supplementary Fig. S4B).

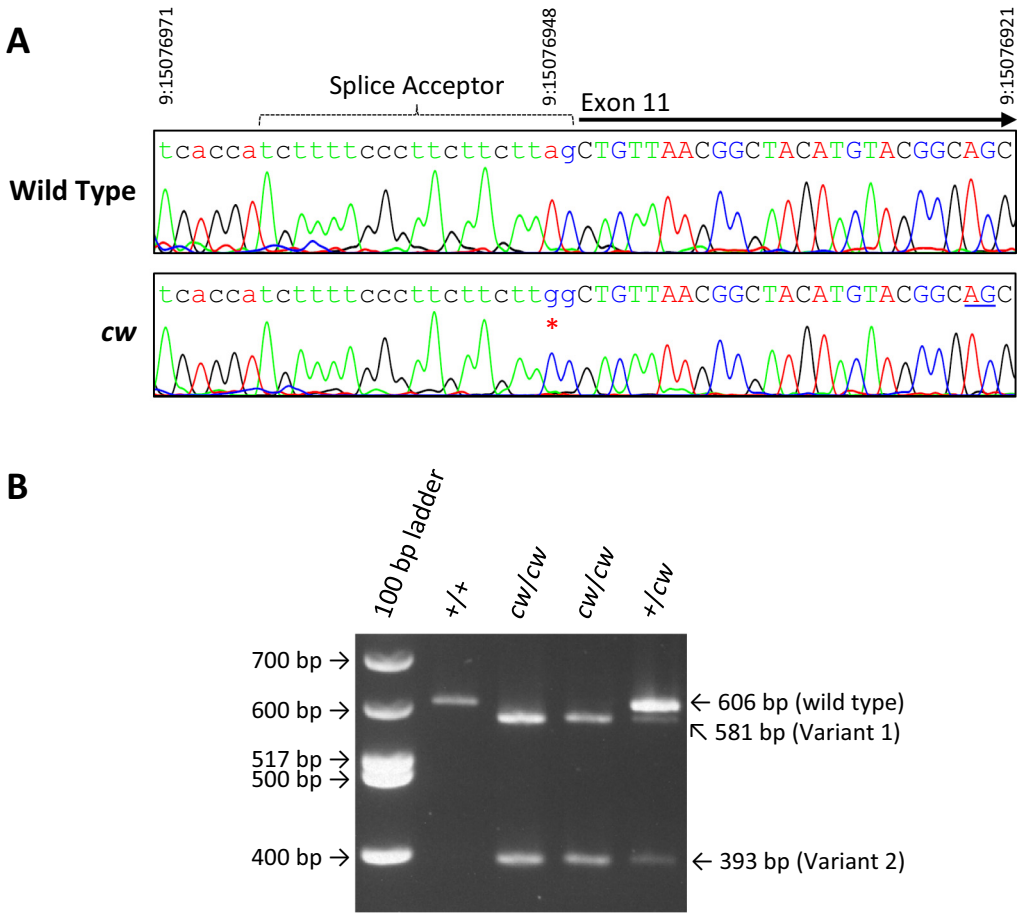

Fig. 4. Comparison of *Hephl1* in wild type and *cw/cw* mutant mice. (A) All coding regions were sequenced in wild type and in *cw/cw* mutant genomic DNA, but only a single difference, at the Intron 10–11 to Exon 11 boundary was found. Shown here are nucleotides 9:15076971 to 9:15076921 from reference sequence GRCm38.p6 (EMGS 2019); with intronic sequences in lower case, exonic sequences in upper case. The pyrimidine-rich tract and the 5′-AG-3′ dinucleotide that compose the standard splice-acceptor signal are indicated over the sequence labeled wild type. The A-to-G substitution found in *cw/cw* mutants (at position 9:15076948) is indicated by a red asterisk on the sequence labeled *cw*. (B) Total RNA isolated from wild type, homozygous mutant and heterozygous tail skin was copied into cDNA, and PCR amplified using primers that annealed within Exons 9 and 12 of *Hephl1*. The 606 bp length (shown here) and sequence (see Fig. S2A) of the amplimer copied from wild type (+/+) cDNA was that expected for the normal splicing of Exons 9 through 12. By contrast, amplification of cDNA derived from mutant (*cw/cw*) skin yielded two different-sized products, of 581 bp (Variant 1) and 397 bp (Variant 2), in about an equal abundance. These variant, *cw*-specific PCR products were isolated and sequenced, as shown in Fig. S2B and 2C, respectively. Notably, since Variant 1 generates an early stop codon, it is likely to be the target of nonsense-mediated decay [4], and so it may be transcribed at an initially higher level than Variant 2. Amplification of *Hephl1* sequences from cDNAs derived from heterozygous (+/*cw*) skin yielded all three product sizes. While the Variant 2 transcript should be stable (since it is predicted to be fully translated), it appears much less abundant than the wild type transcript in the cDNA pool based on heterozygous skin. (For interpretation of the references to colour in this figure legend, the reader is referred to the web version of this article.)

4. Discussion

4.1. The mouse cw mutations are mutant alleles of Hephl1

We have taken a positional-candidate approach to assign the classic *cw* mutation in mice to a splice-acceptor defect in the *Hephl1* gene. Our identification of a second, distinct, allele-specific *Hephl1* defect (a frameshift-inducing, single-base insertion) associated with the cw^{2J} mutation strongly supports this single-gene assignment. We therefore recommend that these curly-whiskers mutations be formally renamed "hephaestin-like 1; curly whiskers" (abbreviated $Hephl1^{cw}$), and "hephaestin-like 1; curly whiskers 2 Jackson" (abbreviated $Hephl1^{cw\text{-}2J}$). We suggest that the $Hephl1^{cw\text{-}2J}$ mutation occurred spontaneously on the B10.SM $H2^{v}$ $H2\text{-}T18^{b}$/(70NS)Sn/J background at least by 1983 (since both the archived DNA samples we analyzed are homozygous for the A insertion in Exon 14), and appears to have become fixed in that strain by its initial cryopreservation in 1999 (since all 39 mice reconstituted for us in 2018 displayed curly whiskers).

Because we restricted our DNA-sequence analysis to *Hephl1* coding regions, only, it remains formally possible that the mutant curly-whiskers phenotype could require additional, unidentified defect(s) in the critical region that work in combination with the *Hephl1* defects that we have described. While we think that such a "two-hit" mechanism is highly unlikely, we note that this model will be explicitly tested when mice homozygous for discrete, engineered variants of *Hephl1*, such as have already been produced (see [36,31,25]) or can be generated *de novo* by gene editing, are phenotypically evaluated.

4.2. Structure and function of Hephl1, and its mutant isoforms

Hephl1 encodes one of three muticopper feroxidases (in addition to hephaestin, *Heph*, and ceruloplasmin, *Cp*) that facilitate iron transport in a variety of tissues and display mostly distinct expression patterns in mammals [5]. The membrane-bound Hephl1 ferroxidase has 6 cupredoxin domains, with binding sites for 6 copper ions. Three of the copper ions form a trinuclear center at the interface of Domains 1 and 6, while the other three form mononuclear centers, and are organized in Domains 2, 4, and 6. In addition, Domain 6 includes a predicted iron-binding site, and is followed by a transmembrane domain [5]. The splice-acceptor defect that we have found associated with *cw* causes omission of Exon 11 from the mature transcript (designated splice Variant 2 in the text), and the resulting mutant $Hephl1^{cw}$ protein is predicted to lack 71 amino acids normally found in Domain 4, but the downstream reading frame is unaltered. By contrast, the frameshifted variants we described (the $Hephl1^{cw}$-specific splice Variant 1 and the $Hephl1^{cw\text{-}2J}$ transcript), since they encode early stop codons, are likely to be eliminated by nonsense-mediated decay [4]. Even if these truncated protein products were produced, they would lack Domains 5 and 6 (including the iron-binding site), and the C-terminal, membrane-spanning domain, and therefore are not expected to contribute any membrane-bound ferroxidase function at all. Hephaestin-like 1's role in iron nutrition and homeostasis is not well understood, but our assignment of two, allelic, curly-whiskers mouse mutants to *Hephl1* should help to set-the-stage for the needed molecular and whole-animal studies.

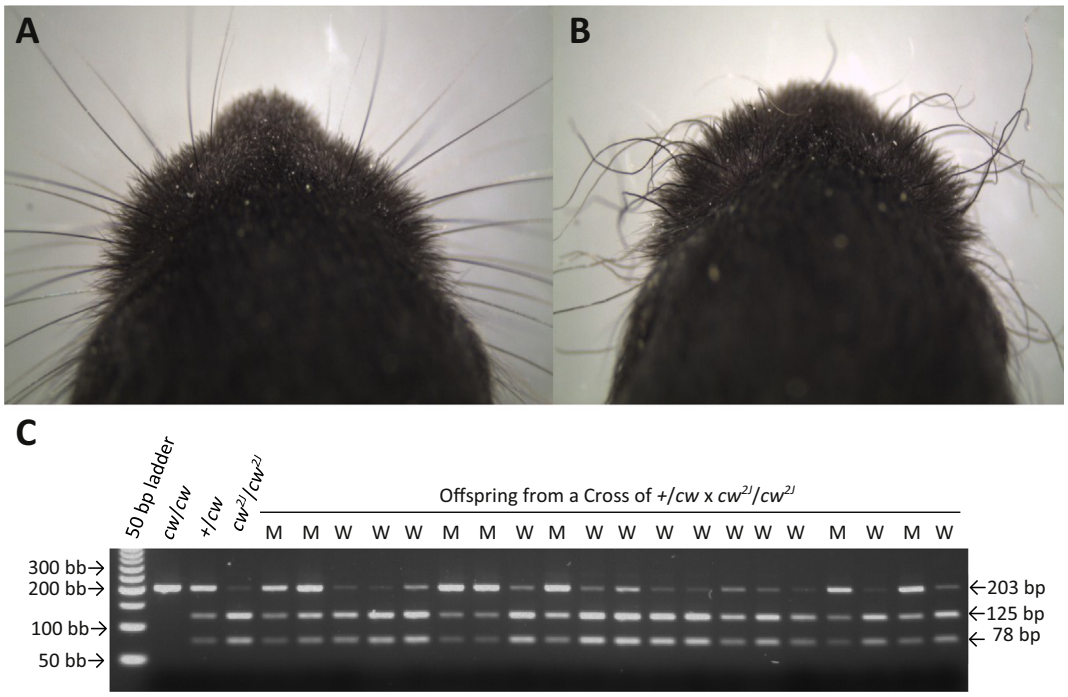

Fig. 5. Phenotype and genotype of mice from a cross of +/*cw* with curly-whiskered B10.SM *H2*^{v} *H2-T18*^{b}/(70NS)Sn/J mice (*i.e.*, Cross 4 in Table 1). This cross produced 20 offspring, 13 with straight whiskers and 7 with curly whiskers. The snout of a typical straight-whiskered mouse (A) and a typical curly-whiskered mouse (B) are shown at 2 weeks of age. This result suggests that the mutation that causes hair-curling in the B10.SM *H2*^{v} *H2-T18*^{b}/(70NS)Sn/J strain is recessive, and that this mutation is an allele of *cw* that we hereby designate *cw*^{2J}. (C) To confirm that all non-complementing, mutant offspring from this cross (labeled M) inherited one copy of *cw*, and that the phenotypically wild type offspring (labeled W) inherited a *cw*$^{+}$ allele instead, a 203 bp amplimer that included the site of the *Hephl1*, splice-acceptor defect associated with *cw* was produced for each mouse, and tested for sensitivity to *Alu*I digestion. By this assay (see Fig. S2), amplimers derived from *cw* templates are resistant to cleavage, while amplimers based on other templates are cut into 125 and 78 bp fragments.

Table 1
Initial crosses of curly-whiskered, B10.SM *H2*^{v} *H2-T18*^{b}/(70NS)Sn/J males.

Cross	Female partner strain (*cw* genotype)	Offspring phenotype	
		Wild type	Curly
1	C57BL/10 (+/+)	8	0
2	CWD/LeJ (*cw/cw*)	0	12
3	CWD.D2 (*cw/cw*)	0	19
4	CWD.D2 (+/*cw*)	13	7

Males of the B10.SM *H2*^{v} *H2-T18*^{b}/(70NS)Sn/J strain, all showing curly whiskers, were crossed with female mice, as indicated. The resulting offspring were assessed for their whisker phenotype at weaning. The result of Cross 1 suggests that the mutant hair phenotype displayed by B10.SM males is generated by homozygosity for a recessive mutation. The results of Crosses 2–4 show that this recessive mutation does not complement the *cw* mutation. We therefore designate the recessive mutation that arose on the B10.SM background curly whiskers-2 Jackson, abbreviated *cw*^{2J}. Typical wild type and mutant pups from Cross 4 are shown in Fig. 5. The number of wild type and mutant offspring from Cross 4 is not different from the 1:1 ratio expected for a test cross ($X^2 = 1.8$; $P > .17$).

Segregation data shown in Fig. S1 and in Fig. 2 suggest that the *Hephl1*^{cw} allele does not negatively impact general viability in homozygotes, at least by weaning age (when our testcross offspring were counted). This may suggest that Hephl1 is not an essential protein, or instead may indicate that the Hephl1^{cw} isoform translated from transcripts that skip Exon 11—despite lacking 71 amino acids in Domain 4—might be normally located in the cell membrane and might retain some "leaky" ferroxidase function. While we have collected only limited segregation data from *Hephl1*$^{cw\text{-}2J}$ testcrosses, to date, our current tally does show a small deficit of mutants compared to wild type (perhaps indicating that *Hephl1*$^{cw\text{-}2J}$ may control a more severe phenotype than *Hephl1*^{cw}), but these counts are still modest ($N = 106$) and the deviation from the 1 wild:1 mutant testcross ratio expected for full viability is not statistically significant ($P > .12$). Of course, any predictions regarding Hephl1^{cw} and Hephl1$^{cw\text{-}2J}$ protein structure, location, and function need to be explicitly tested, ideally, side-by-side with a *bone fide* null mutant, as are readily available from multiple sources (see [36,31,25], for example).

4.3. *Hephl1 impairment causes pili torti*

Our selection of *Hephl1* as a likely positional candidate for *cw* was largely due to the association of kinky, brittle hair (*pili torti*) with generalized copper deficiency, as in Menkes disease, an X-linked recessive disorder (resulting from defects in the copper-transport protein ATP7A) whose myriad clinical features are thought to result from the dysfunction of several copper-dependent enzymes (OMIM, entry #309400, [27]). While several cuproenzymes have been proposed to account for the various features of the disorder (tyrosinase for depigmentation of hair and skin, lysyl oxidase for connective tissue defects, cytochrome c oxidase for hypothermia, and ascorbate oxidase for skeletal demineralization, for example; reviewed by [23]), this report is the first to implicate hephaestin-like 1 in, at least, the kinky-hair feature of Menkes disease and the related occipital horn syndrome (OMIM, entry #304150, [26]). Other aspects of these disease syndromes may also be owing to reduced Hephl1 activity, since *Hephl1* is expressed in some of the same tissues impacted by these conditions (including the retina [17,19], synovial membranes [1], and in the cardiovascular, connective, urinary and nervous systems [5]), but these tissues have not yet been examined in any detail in the curly-whiskers mouse mutants. In any case, the animal models we have now causally ascribed to *Hephl1*-deficiency should facilitate the functional dissection of these complex, pleiotropic human disorders, and hopefully advance the

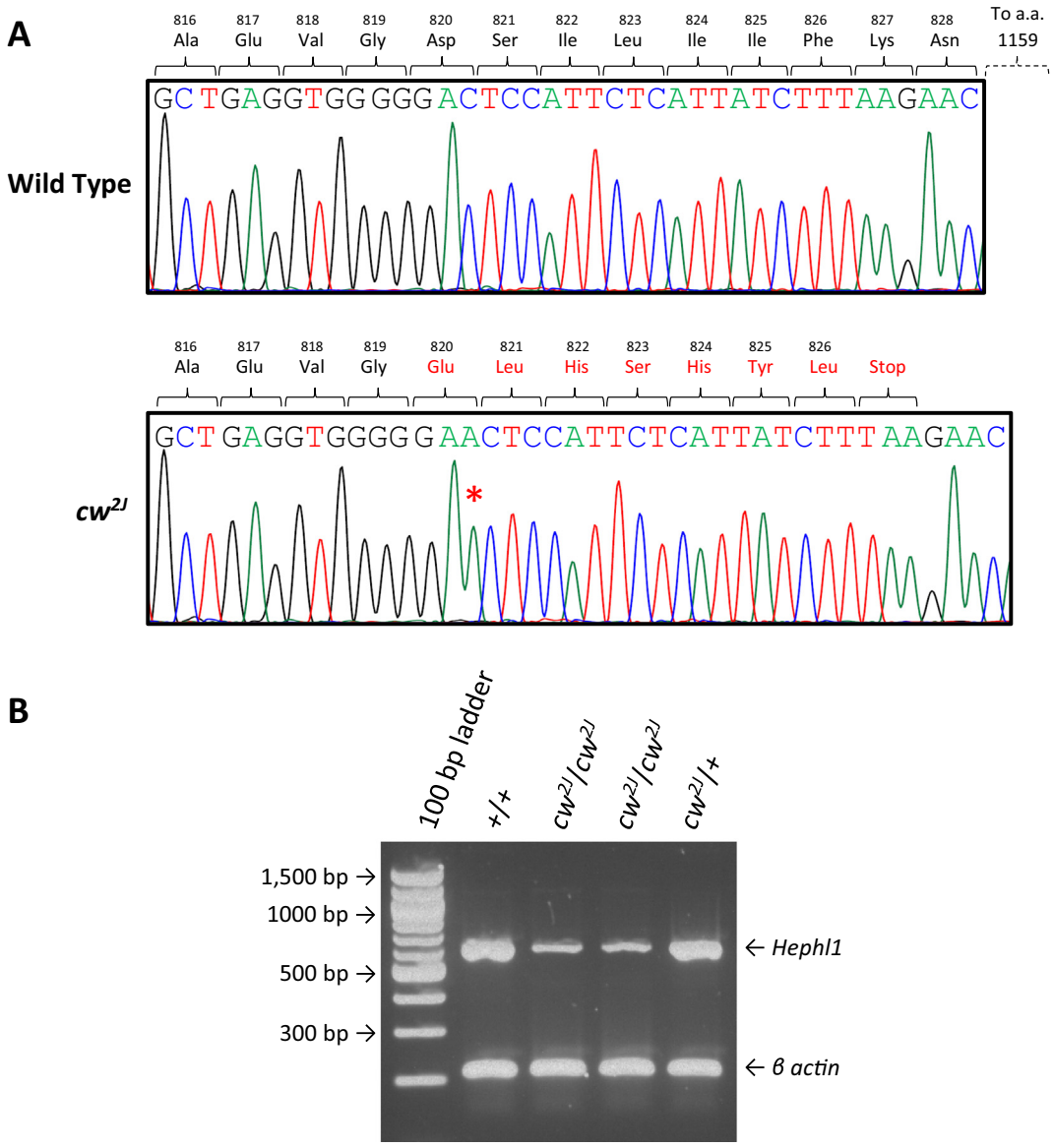

Fig. 6. Comparison of *Hephl1* in wild type and cw^{2J}/cw^{2J} mutant mice. (A) All coding regions were sequenced in wild type and in cw^{2J}/cw^{2J} mutant genomic DNA, but only a single difference, in Exon 14, was found. This mutation, the insertion of a single A residue in cw^{2J}/cw^{2J} mutants compared to wild type, is indicated with a red asterisk on the sequence labeled cw^{2J}. The sequence shown here includes nucleotides 9:15067163 to 9:15067125, from reference sequence GRCm38.p6 (EMGS 2019). This insertion is predicted to shift the translational reading frame on mutant transcripts, generating seven novel amino acids (residues 820–826, shown in red) followed by an early, out-of-frame stop codon. (B) Total RNA isolated from wild type, homozygous cw^{2J}/cw^{2J} mutant or heterozygous tail skin was copied into cDNA, and PCR amplified using one primer pair specific to *Hephl1* together with a second primer pair specific to the β actin gene (*Actb*). The resulting amplimers were then separated by gel electrophoresis. While the levels of *Actb* signal amplified from the cDNAs derived from each different genotype is essentially equivalent, *Hephl1* transcripts amplified from cw^{2J}/cw^{2J} templates appear markedly less abundant compared to amplimers based on wild type cDNAs. It is likely that this variant transcript, which cannot be fully translated, is unstable due to nonsense-mediated mRNA decay [4]. (For interpretation of the references to colour in this figure legend, the reader is referred to the web version of this article.)

development of treatments for at least some aspects of the syndromes they generate.

4.4. Do these curly-whiskers mutants generate skin-graft histoincompatibility?

We remain especially curious to learn whether $Hephl1^{cw}$ and/or $Hephl1^{cw\text{-}2J}$, like the now-extinct cw^{thd} allele, might also generate an immunological "gain" or "loss" of antigenicity that can be detected by skin-graft-exchange assay, for example. Classically, mutations that create such heritable barriers to graft compatibility have identified the so-called minor histocompatibility (*H*) loci [28], which currently number in excess of 60. However, mutations that affect both transplantation acceptance and a distinct developmental function are quite rare. We know of only one other example, the recessive *H-mshi* mutation (for "male sterility and histoincompatibility", [37]) which causes aspermia in homozygous males, but was initially discovered as the loss of a cell-surface antigen, such that tail skin from +/+ mice is rejected by (otherwise genetically-matched) *mshi/mshi* mutants, which recognize the $mshi^{+}$ antigen as "foreign" [13,22,30,34].

This sort of phenotypic complexity interests us for several reasons. First, we anticipate that the antigenicity of the gene product might easily be exploited to provide another molecular "handle" for gaining access to the molecular physiology controlled by *Hephl1*. Second, mutations that control seemingly unrelated functions (histocompatibility and sperm production or hair development, for example), offer an

opportunity to dissect the cause of such compelling pleiotropy, a phenomenon of enduring interest in formal genetics. Third, it seems possible (even likely) that the study of antigen-altering mutations could reveal much about human disease phenotypes that might involve autoimmune reactions against the orthologous protein products (see [16]). Finally, we believe it is still important to identify and characterize new minor *H* loci, so that their individual and collective significance in graft transplantation can be formally assessed.

To prepare to conduct such histogenic assessments, we have been developing genetically "pure" mouse stocks that segregate for *Hephl1*$^{+}$ and each recessive curly-whiskers mutation. These inbred strains should allow the production of homozygous mutant, heterozygous, and homozygous wild-type subjects on the otherwise uniform genetic background that is required for single-gene, allograft analysis. To develop a line that segregates for *Hephl1*$^{+}$ and *Hephl1*^{cw}, we have crossed CWD/LeJ homozygotes, *Hephl1*^{cw} *Myo5a*^{d}/*Hephl1*^{cw} *Myo5a*^{d}, with strain DBA/2J (the original source of the *Myo5a*^{d} in the CWD/LeJ strain). The resulting *Hephl1*$^{+}$ *Myo5a*^{d}/ *Hephl1*^{cw} *Myo5a*^{d} F_1 offspring (with straight vibrissae) were then crossed back to CWD/LeJ mutants to produce *Hephl1*^{cw}/*Hephl1*$^{+}$ heterozygotes that were crossed back to CWD/LeJ, and so on. This segregating congenic line, named CWD.D2-*Hephl1*$^{+}$/*Hephl1*^{cw}, is currently at N_{13}. To develop a stock segregating for *Hephl1*$^{+}$ and *Hephl1*$^{cw\text{-}2J}$, we crossed B10.SM *H2*^{v} *H2-T18*^{b}/(70NS)Sn/J-*Hephl1*$^{cw\text{-}2J}$ mutant males to C57BL/10SnJ females, and the F_1 offspring were crossed back to C57BL/10SnJ. Heterozygous offspring from this cross, identified by the *Mly*I-sensitivity test we described, were crossed back to C57BL/10SnJ, and so on, to create a segregating inbred strain named C57BL/10SnJ-*Hephl1*$^{+}$/*Hephl1*$^{cw\text{-}2J}$ (currently at N_5) that will be, essentially, co-isogenic. While primarily designed for the immunogenetic analyses that we anticipate performing, these uniform, inbred stocks should also be ideal for making other well-controlled molecular and functional comparisons among the various *Hephl1* genotypes.

4.5. Positional cloning: the end of an era

In recent years, modern methods (like whole-genome DNA sequencing) have supplanted positional cloning (sometimes called "reverse genetics") as an approach for making causative-gene assignments for spontaneous mutations, in both mice and man [10,18,35]. And even if this powerful new method works best when the natural variant under study has had some prior positional characterization, genetic mapping as a means to gain initial access to gene structure and function appears (perhaps with this report) to have become outdated. Indeed, the current ease with which genetic variants can be deliberately and precisely engineered (by gene targeting or gene editing, for example), infers that even spontaneous mutations—once the *only* source genetic variation—are no longer particularly prized. We would argue, instead, that natural mouse variants (like curly whiskers) often contribute a critically informative part of an allelic series, where they can frequently offer a unique perspective into the pathobiology of inherited human disorders, which similarly result from leaky, pleiotropic and often surprising spontaneous mutations.

Supplementary data to this article can be found online at https://doi.org/10.1016/j.ymgmr.2019.100478.

Competing interests

The authors declare no competing interests.

Acknowledgements

The authors thank: CCSU students Anthony Renzi, Ondine Fraher, Erica Negrini and Shauna-Kay Nugent for assistance with marker typing and preparation of PCR-based amplimers for primer-extension sequencing; Dr. Cathleen Lutz (Rare and Orphan Disease Center, The Jackson Laboratory, Bar Harbor, ME) for help with importation of the B10.SM *H2*^{v} *H2-T18*^{b}/(70NS)Sn/J strain to CCSU; and Ms. Mary Mantzaris for excellent animal care. This work was supported by research grants from the Connecticut State Colleges and Universities System, and the National Institute of Allergy and Infectious Disease of the National Institutes of Health under Award Number R03AI144350. The content is solely the responsibility of the authors and does not necessarily represent the official views of the National Institutes of Health.

References

[1] M. Bhattacharjee, R. Sharma, R. Goel, L. Balakrishnan, S. Renuse, J. Advani, S.T. Gupta, R. Verma, S.M. Pinto, N.R. Sekhar, B. Nair, T.S.K. Prasad, H.C. Harsha, R. Jois, S. Shankar, A. Pandey, A multilectin affinity approach for comparative glycoprotein profiling of rheumatoid arthritis and spondyloarthropathy, Clin. Proteomics 10 (2013) 11.

[2] J. Buis, Y. Wu, Y. Deng, J. Leddon, G. Westfield, M. Eckersdorff, J.M. Sekiguchi, S. Chang, D.O. Ferguson, *Mre11* nuclease activity has essential roles in DNA repair and genomic stability distinct from ATM activation, Cell 135 (2008) 85–96.

[3] M.A. Carmell, A. Girard, H.J.G. van de Kant, D. Bourc'his, T.H. Bestor, D.G. de Rooij, G.J. Hannon, MIMI2 is essential for spermatogenesis and repression of transposons in the mouse male germline, Dev. Cell 12 (2007) 503–514.

[4] Y.-F. Chang, J.S. Imam, M.F. Wilkinson, The nonsense-mediated decay RNA surveillance pathway, Annu. Rev. Biochem. 76 (2007) 51–74.

[5] H. Chen, Z.K. Attieh, B.A. Syed, Y.-M. Kuo, V. Stevens, B.K. Fuqua, H.S. Andersen, C.E. Naylor, R.W. Evans, L. Gambling, R. Danzeisen, M. Bacouri-Haidar, J. Usta, C.D. Vulpe, H.J. McArdle, Identification of zyklopen, a new member of the vertebrate multicopper ferroxidase family, and characterization in rodents and human cells, J. Nutr. 140 (2010) 1728–1735.

[6] F.S. Collins, Positional cloning moves from perditional to traditional, Nat. Genet. 9 (1995) 347–350.

[7] G. Diez-Roux, S. Banfi, M. Sultan, L. Geffers, S. Anand, D. Rozado, A. Magen, E. Canidio, M. Pagani, I. Peluso, N. Lin-Marq, M. Koch, M. Bilio, I. Cantiello, R. Verde, C. De Masi, S.A. Bianchi, J. Cicchini, E. Perroud, S. Mehmeti, E. Dagand, S. Schrinner, A. Nürnberger, K. Schmidt, K. Metz, C. Zwingmann, N. Brieske, C. Springer, A.M. Hernandez, S. Herzog, F. Grabbe, C. Sieverding, B. Fischer, K. Schrader, M. Brockmeyer, S. Dettmer, C. Helbig, V. Alunni, M.A. Battaini, C. Mura, C.N. Henrichsen, R. Garcia-Lopez, D. Echevarria, E. Puelles, E. Garcia-Calero, S. Kruse, M. Uhr, C. Kauck, G. Feng, N. Milyaev, C.K. Ong, L. Kumar, M. Lam, C.A. Semple, A. Gyenesei, S. Mundlos, U. Radelof, H. Lehrach, P. Sarmientos, A. Reymond, D.R. Davidson, P. Dollé, S.E. Antonarakis, M.L. Yaspo, S. Martinez, R.A. Baldock, G. Eichele, A. Ballabio, A high-resolution anatomical atlas of the transcriptome in the mouse embryo, PLoS Biol. 9 (2011) e1000582.

[8] W.F. Dietrich, J. Miller, R. Steen, M.A. Merchant, D. Damron-Boles, Z. Husain, R. Dredge, M.J. Daly, K.A. Ingalls, T.J. O'Connor, A comprehensive genetic map of the mouse genome, Nature 380 (1996) 149–152, https://doi.org/10.1038/380149a0.

[9] Ensembl Mouse Genome Server (EMGS), the European Bioinformatics Institute (EBI), the Welcome Trust Sanger Institute (WTSI), Release 95, Available from: www.ensembl.org.

[10] H. Fairfield, A. Srivastava, G. Ananda, R. Liu, M. Kircher, A. Lakshminarayana, B.S. Harris, S.Y. Karst, L.A. Dionne, C.C. Kane, M. Curtain, M.L. Berry, P.F. Ward-Bailey, I. Greenstein, C. Byers, A. Czechanski, J. Sharp, K. Palmer, P. Gudis, W. Martin, A. Tadenev, L. Bogdanik, C.H. Pratt, B. Chang, D.G. Schroeder, G.A. Cox, P. Cliften, J. Milbrandt, S. Murray, R. Burgess, D.E. Bergstrom, L.R. Donahue, H. Hamamy, A. Masri, F.A. Santoni, P. Makrythanasis, S.E. Antonarakis, J. Shendure, L.G. Reinholdt, Exome sequencing reveals pathogenic mutations in 91 strains of mice with Mendelian disorders, Genome Res. 25 (2015) 948–957.

[11] D.S. Falconer, J.H. Isaacson, Curly-whiskers and its linkage with tail-kinks in linkage group II of the mouse, Genet. Res. Camb. 8 (1966) 111–113.

[12] D.S. Falconer, J.H. Isaacson, Linkage of curly-whiskers, short ear and tail-kinks, Mouse News Letter 27 (1962) 30.

[13] A.L. Hildebrandt, A.M. Cantwell, M.C. Rule, T.R. King, The H-mshi antigen is conserved among standard BALB/cBy, C57BL/6J, and wild-derived CAST/Ei and SPRET/Ei inbred strains of mice, Immunogenetics 49 (1999) 666–672.

[14] J.W. Homeister, A.D. Thall, B. Petryniak, P. Maly, C.E. Rogers, P.L. Smith, R.J. Kelly, K.M. Gersten, S.W. Askari, G. Cheng, G. Smithson, R.M. Marks, A.K. Misra, O. Hindsgual, U.H. von Andrian, J.B. Lowe, The alpha (1,3) fucosyltransferases FucT-IV and FucT-VII exert collaborative control over selectin-dependent leukocyte recruitment and lymphocyte homing, Immunity 15 (2001) 115–126.

[15] N. Inoue, M. Ikawa, A. Isotani, M. Okabe, The immunoglobulin superfamily protein Izumo is required for sperm to fuse with eggs, Nature 434 (2005) 234–238.

[16] S. Karpati, M. Sardy, K. Nemeth, B. Mayer, N. Smyth, M. Paulsson, H. Traupe, Transgutamonases in autoimmune and inherited skin diseases: the phenomena of epitope spreading and functional compensation, Exp. Dermatol. 27 (2018) 807–814.

[17] M.S. Kim, S.M. Pinto, D. Getnet, R.S. Nirujogi, S.S. Manda, R. Chaerkady, A.K. Madugundu, D.S. Kelkar, R. Isserlin, S. Jain, J.K. Thomas, B. Muthusamy, P. Leal-Rojas, P. Kumar, N.A. Sahasrabuddhe, L. Balakrishnan, J. Advani, B. George, S. Renuse, L.D. Selvan, A.H. Patil, V. Nanjappa, A. Radhakrishnan, S. Prasad, T. Subbannayya, R. Raju, M. Kumar, S.K. Sreenivasamurthy, A. Marimuthu,

G.J. Sathe, S. Chavan, K.K. Datta, Y. Subbannayya, A. Sahu, S.D. Yelamanchi, S. Jayaram, P. Rajagopalan, J. Sharma, K.R. Murthy, N. Syed, R. Goel, A.A. Khan, S. Ahmad, G. Dey, K. Mudgal, A. Chatterjee, T.C. Huang, J. Zhong, X. Wu, P.G. Shaw, D. Freed, M.S. Zahari, K.K. Mukherjee, S. Shankar, A. Mahadevan, H. Lam, C.J. Mitchell, S.K. Shankar, P. Satishchandra, J.T. Schroeder, R. Sirdeshmukh, A. Maitra, S.D. Leach, C.G. Drake, M.K. Halushka, T.S. Prasad, R.H. Hruban, C.L. Kerr, G.D. Bader, C.A. Iacobuzio-Donahue, H. Gowda, A. Pandey, A draft map of the human proteome, Nature 509 (2014) 575–581.

[18] C.-S. Ku, D.N. Cooper, G.P. Patrinos, The rise and rise of exome sequencing, Public Health Genom. 19 (2016) 315–324.

[19] Y. Kuo, Z. Attieh, H. Chen, B. Syed, J. Gitschier, H.J. McArdle, C. Vulpe, Zyklopen, a new member of the multi-copper ferroxidase family, is expressed in multiple tissues, Am. J. Hematol. 82 (2007) 510.

[20] E.P. Les, J.B. Roths, New mutation, Mouse News Letter 53 (1975) 34.

[21] M.F. Lyon, J. Butler, Position of centromere in linkage groups II & IX, Mouse News Letter 37 (1967) 30.

[22] D.R. Magnan, D.V. Spacek, N. Ye, Y.-C. Lu, T.R. King, The male sterility and histoincompatibility (*mshi*) mutation in mice is a natural variant of microtubule-associated protein 7 (*Mtap7*), Mol. Genet. Metabol. 97 (2009) 155–162.

[23] J.H. Menkes, Kinky hair disease: twenty five years later, Brain and Development 10 (1988) 77–79.

[24] Mouse Genome Database (MGD), Mouse Genome Database Group: The Mouse Genome Informatics Website, The Jackson Laboratory, Bar Harbor ME, 2019 Available from https://www.informatics.jax.org.

[25] Mutagenetix Database (MD), B. Beutler and et al., Center for the Genetics of Host Defense, UT Southwestern, Dallas, TX. Accessed April 2019 URL: https://mutagenetix.utsouthwestern.edu

[26] Online Mendelian Inheritance in Man (OMIM), McKusick-Nathans Institute of Genetic Medicine, Johns Hopkins University, Baltimore, MD, 2012 MIM Number: #304150 (occipital horn syndrome) Retrieved March 2019, from https://omim.org.

[27] Online Mendelian Inheritance in Man (OMIM), McKusick-Nathans Institute of Genetic Medicine, Johns Hopkins University, Baltimore, MD, 2016 MIM Number: #309400 (Menkes disease) Retrieved March 2019, from https://omim.org.

[28] D.C. Roopenian, E.-Y. Choi, A. Brown, The immunogenomics of minor histocompatibility antigens, Immunol. Rev. 190 (2002) 86–94.

[29] J.B. Roths, Alleleism of tail hair depletion with curly whiskers, Mouse News Lett. 58 (1978) 50.

[30] M.C. Rule, R.J. Mutcherson II, A.D. Foss, T.K.-X. Nguyen, K.A. Myrie, T.R. King, Mouse male sterility and histocompatibility (*mshi*) maps between the *D10Mit51/168/212* cluster and *D10Mit213*, Mamm. Genome 10 (1999) 447–450.

[31] W.C. Skarnes, B. Rosen, A.P. West, M. Koutsourakis, W. Bushell, V. Iyer, A.O. Mujica, M. Thomas, J. Harrow, T. Cox, D. Jackson, J. Severin, P. Biggs, J. Fu, M. Nefedov, P.J. de Jong, A.F. Stewart, A. Bradley, A conditional knockout resource for the genome-wide study of mouse gene function, Nature 474 (2011) 337–342.

[32] M.F. Santiago, J. Veliskova, N.K. Patel, S.E. Lutz, D. Caille, A. Charollais, P. Meda, E. Scemes, Targeting pannexin1 improves seizure outcome, PLoS One 6 (2011) e25178.

[33] C. Toms, H. Jessup, C. Thompson, D. Baban, K. Davies, F. Powrie, *Gpr83* expression is not required for the maintenance of intestinal immune homeostasis and regulation of T-cell-dependent colitis, Immunlogy 125 (2008) 302–312.

[34] J.P. Turner, J.E. Carpentino, A.M. Cantwell, A.L. Hildebrandt, K.A. Myrie, T.R. King, Molecular genetic mapping of the mouse male sterility and histoincompatibility (*mshi*) mutation on proximal Chromosome 10, Genomics 39 (1997) 1–7.

[35] J.A. Veltman, H.G. Brunner, De novo mutations in human genetic disease, Nat. Rev. 13 (2012) 565–575.

[36] C. Vulpe, Direct Data Submission for Flowed and Knock-out Zyklopen (*Hephl-1*) Alleles. *MGI Direct Data Submission*, MGI Ref. ID: J:210156. The Mouse Genome Informatics Website, The Jackson Laboratory, Bar Harbor, ME, 2014 (Available from, https://www.informatics.jax.org.

[37] P.F. Ward-Bailey, K.R. Johnson, M.A. Handel, B.S. Harris, M.T. Davisson, Male sterility and histoincompatibility (*mshi*): a new mutation on mouse Chromosome 10, Mamm. Genome 7 (1996) 793–797.